



# Surface functionalization of acrylic based photocrosslinkable resin for 3D printing applications



A. Ronca<sup>a,\*</sup>, F. Maiullari<sup>b</sup>, M. Milan<sup>b</sup>, V. Pace<sup>b</sup>, A. Gloria<sup>a</sup>, R. Rizzi<sup>b</sup>, R. De Santis<sup>a</sup>, L. Ambrosio<sup>a</sup>

<sup>a</sup> Institute of Polymers, Composites and Biomaterials – National Research Council (IPC-CNR), Italy

<sup>b</sup> Institute of Cellular Biology and Neurobiology – National Research Council (IBCN-CNR), Italy

## ARTICLE INFO

### Article history:

Received 28 February 2017

Received in revised form

11 April 2017

Accepted 12 April 2017

Available online 21 April 2017

## ABSTRACT

The limited number of resins, available for stereolithography applications, is one of the key drivers in research applied to rapid prototyping. In this work an acrylic photocrosslinkable resin based on methyl methacrylate (MMA), butyl methacrylate (BMA) and poly(ethylene glycol) dimethacrylate (PEGDA) was developed with different composition and characterized in terms of mechanical, thermal and biological behaviour. Two different systems have been developed using different amount of reagent. The influence of every components have been evaluated on the final characteristic of the resin in order to optimize the final composition for applications in bone tissue engineering. The crosslinked materials showed good mechanical properties and thermal stabilities and moreover cytotoxicity test confirms good biocompatibility with no cytotoxic effect on cells metabolism. Moreover two different treatments have been proposed, using fetal bovine serum (FBS) and methanol (MeOH), in order to improve cell recognition of the surfaces. Samples threatened with MeOH allow cell adhesion and survival, promoting spreading, elongation and fusion of C2C12 muscle myoblast cells.

© 2017 The Authors. Production and hosting by Elsevier B.V. on behalf of KeAi Communications Co., Ltd. This is an open access article under the CC BY-NC-ND license (<http://creativecommons.org/licenses/by-nc-nd/4.0/>).

## 1. Introduction

In reconstructive surgery 3D structures are developed and fabricated to play specific roles including scaffolds as temporary spacers [1,2], system for controlled drug release [3] and biodegradable biomaterials for tissue engineering [4]. These biomaterials are necessary to replace bone as a result of bone injuries due to trauma, bone tissue loss after tumor surgery, and congenital bone malformations or in providing a temporary spacer in the case of bone implant failure due to infection [5–8]. Central role in tissue engineering is played by the scaffold that have to provide a support to the cells and must regulate cell development into complex three-dimensional (3D) structures [9–11]. Stereolithography is considered one of the most versatile method providing the highest accuracy and precision to the final 3D structure [12]. The working principle of stereolithography is based on spatially controlled

solidification of a liquid photo-polymerizable resin. Polymers and composites are widely used for tissue engineering applications due to their low cost, flexibility, and ease of manufacturing. However, their surface properties often do not meet the demands regarding wettability and biocompatibility for cells adhesion and proliferation [13]. For example poly(methyl methacrylate) (PMMA) is an FDA approved synthetic biomaterial widely employed in ophthalmic, orthopaedic and dental applications [14,15]. There are several disadvantages of using PMMA like its brittleness [16] and exothermic temperature risen during polymerization that can lead to necrosis of surrounding tissues and implant failure [17–22]. A variety of literature investigations reported the use of co-polymer based on a combination of methyl-methacrylate and butyl methacrylate (BMA) in order to tune the mechanical and thermal properties of PMMA [23,24]. In this work, in order to synthesize an innovative material for stereolithography applications and to tune the mechanical and biological properties of PMMA, a photocrosslinkable resin based on methyl methacrylate (MMA) and butyl methacrylate (BMA) has been developed using poly(ethylene glycol) dimethacrylate (PEGDA) as crosslinking agent. The mechanical properties of new crosslinked materials were

\* Corresponding author.

E-mail address: [alfredo.ronca@cnr.it](mailto:alfredo.ronca@cnr.it) (A. Ronca).

Peer review under responsibility of KeAi Communications Co., Ltd.

characterized using tensile testing and dynamic mechanical analysis (DMA) while thermal stability was analysed through differential scanning calorimetry (DSC). However both PMMA, PBMA and PEGDA have been presumed to be almost biologically inert due to their relatively low surface energy and lack of biofunctional groups causing a negative effect on cell adhesion and biocompatibility. Moreover, an increasing number of publications have shown that PMMA can give rise to an inflammatory response when implanted in different locations of the body in rats [25], guinea pigs [26] and rabbits [27]. Consequently, it is very difficult to use PMMA as biomaterial for tissue regeneration without modifying its surface in order to improve its cells recognition [28,29]. The enhanced integration of the material with the bioenvironmental would be advantageous particularly related to orthopaedic applications [30,31]. Cell adhesion to and spreading on a biomaterial is, amongst other factors, dependent on the surface wettability of the biomaterial [32]. Schakenraad et al. reported that cells spread poorly on hydrophobic substrata and more extensively on more hydrophilic substrata [33]. Absolom et al. reported a similar dependence on substratum wettability for endothelial cell coverage of the substratum [34]. Van Wachem et al. found that human endothelial cells adhered optimally (in terms of numbers) on moderately wettable polymers [35]. In this work a preliminary study of FBS and methanol (MeOH) treatments on photocrosslinked network has been proposed in order to improve surface wettability and cell recognition of the synthesized materials. Finally, the influence of these treatments on the adhesion, growth and morphology of C2C12 skeletal muscle precursors cells was studied.

## 2. Materials and methods

### 2.1. Materials

Methyl methacrylate (MMA), Butyl methacrylate (BMA), Poly(ethylene glycol) dimethacrylate (PEGDA  $M_w = 550$ ) were obtained from Sigma–Aldrich and used without further purification. Technical grade isopropanol and acetone were obtained from Biosolve (The Netherlands) and they were used as received. Lucirin TPO-L (ethyl-2,4,6-trimethylbenzoylphenylphosphinate) was kindly provided by BASF, Germany. D-MEM, Fetal bovine serum (FBS) and Glutamax was provided by Gibco, USA. Penicilin and streptomycin was provided by EuroClone S.p.a., Italy. C2C12 muscle myoblast cell line was supplied from ATCC® leading biological standards. Human osteoblasts were extracted from human tibia gently donated from Villa Betania Hospital.

### 2.2. Resins preparation and crosslinking

Varying ratios of MMA/BMA (Table 1) monomers were mixed thoroughly with desired amounts of PEGDA as crosslinker and Lucirin TPO as photo-initiator. The amount of the initiator used was fixed, in all cases, to 1 wt% of the total mixture. Monomer resin were synthesized varying the molar ratio of the three component. The component was mechanically stirred for 30 min before polymerization. Throughout this paper, all resins are labelled a System 1 and 2 and their molecular composition are reported in Table 1. The Poly(MMA-co-BMA)-PEGDA network was prepared by radical

photopolymerization of MMA monomers with BMA in the presence of PEGDA ( $M_w = 550$ Da) as crosslinker and Lucirin TPO as photo-initiator. Mixtures of the MMA-BMA monomers, the PEGDA crosslinking oligomer, and the photoinitiator were mixed through magnetic stirring for 30 min and injected into a cylindrical teflon mold. A 365 nm UV lamp (spectroline) were used for the crosslinking process irradiating the resin for 60 min. The prepared networks were taken out from the mold and washed by placing them in 200 mL of a mixture 3/1 isopropanol/acetone. After this primary polymerization stage was completed, the samples were postcured in oven at 90 °C for 24 h to complete the crosslinking reaction. Two different ratios of MMA/BMA monomers were mixed thoroughly with desired amounts of the crosslinker (PEGDA), and the different composition are reported in Table 1. This was accomplished by placing them in a temperature-controlled oven at 90 °C overnight under vacuum. The polymeric system studied is comprised essentially of a methyl methacrylate (MMA) backbone with varying amounts of butyl methacrylate (BMA) co-monomer to provide certain flexibility to the chain. The introduction of PEGDA as crosslinking agent results in the formation of a three-dimensional network as showed in Fig. 1.

### 2.3. Network characterization

#### 2.3.1. Differential scanning calorimetry (DSC)

To assess and characterize the physical properties of the network, disk of 10 mm in diameter were cut from the photocrosslinked film. The glass transition temperature ( $T_g$ ) of the samples were determined with differential scanning calorimetry (DSC, Q1000, TA Instruments). To achieve good sensitivity, three steps were performed. The samples were heated from 30 °C to 90 °C at a constant rate of 10 °C/min. Second, quench the samples to –60 °C after holding at 90 °C for 1 min. And third step, the samples were heated from –60 °C to 100 °C at a constant rate of 2 °C/min. The glass transition temperatures were calculated from the third scan (Fig. 2) and reported in Table 2.

#### 2.3.2. Tensile test

Mechanical tensile testing was performed on “dogbones” shapes samples, according to the ISO D1708, by a uniaxial testing machine (Instron 5566) with a 1 KN load cell using a cross-head speed of 5 mm/min. From the stress–strain curves, the tensile modulus, ultimate tensile strength and elongation-at-break were obtained. For each material set in Table 1, five samples have been tested for every composition ( $n = 5$ ).

#### 2.3.3. Dynamic mechanical analysis

Samples for dynamic mechanical analysis (DMA) were prepared

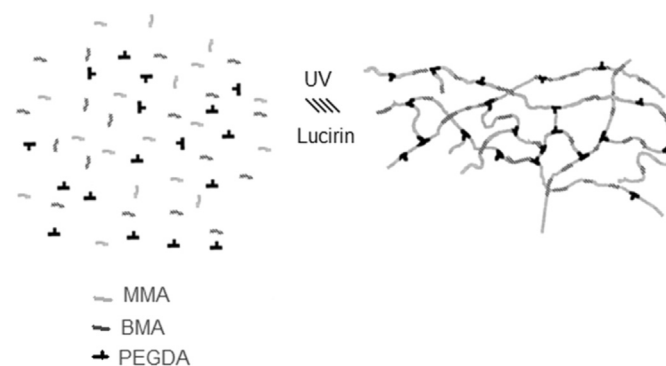


Fig. 1. A simplified model for the structure of the synthesized cross-linked photocrosslinking reaction of the acrylate monomers in presence of PEGDA as crosslinker.

Table 1  
Percentage molar composition (%mol) of system 1 and system 2 resins.

	MMA (% mol)	BMA (% mol)	PEGDA (% mol)
System 1	50	15	35
System 2	70	22	8

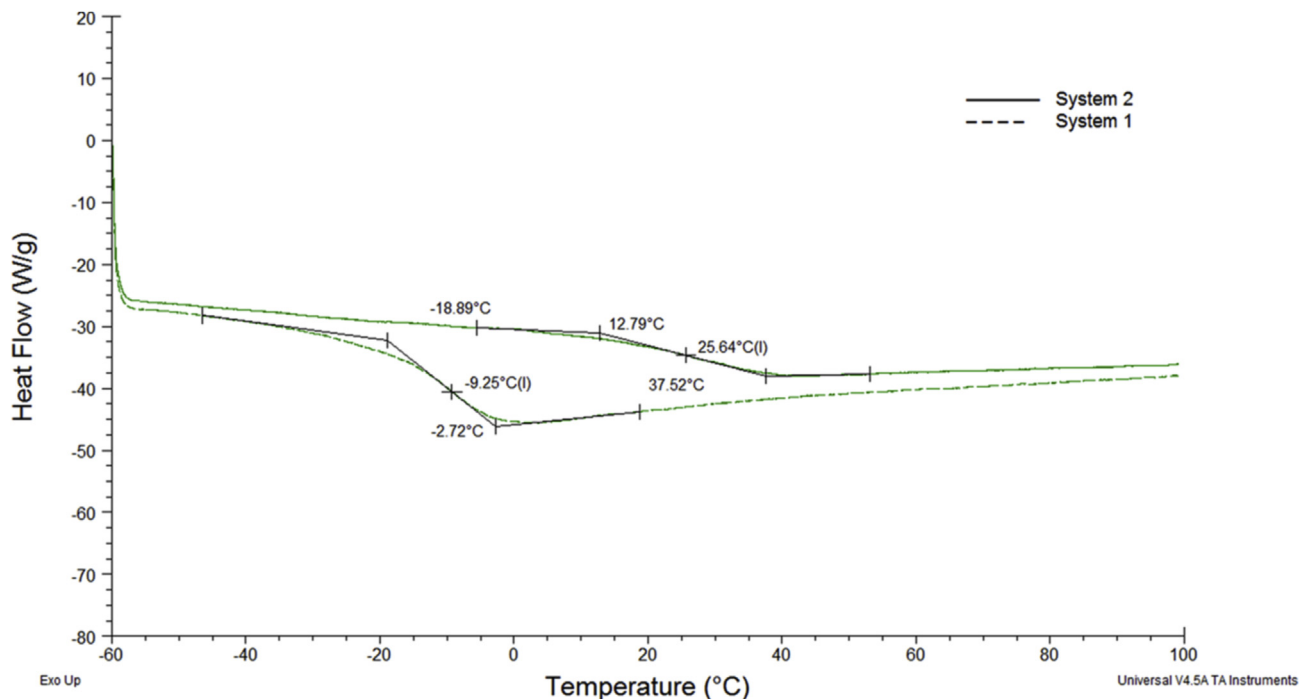


Fig. 2. DSC curves for the two crosslinked network in nitrogen, at a heating rate of 2 °C/min.

Table 2

Mechanical and thermal data from tensile test, DMA and DSC on system 1 and system 2 crosslinked network.

Sample	Tensile test			DMA		DSC
	E' (MPa)	$\epsilon_{\max}$ (%)	$\sigma_{\max}$ (MPa)	E' (T = 25 °C) (MPa)	T <sub>g</sub> (°C)	T <sub>g</sub> (°C)
System 1	32,68	8	2,78	23,91	4,2	-9,12
System 2	260,41	40	10,81	337,79	53,6	30,21

by cutting prismatic specimens of  $10 \times 5 \times 1 \text{ mm}^3$  from a cross-linked film having a thickness of 1 mm. A Tritec 2000 (Triton Technologies) was used in bending loading with strain of 0.01 mm and frequency of 1 Hz. The samples were equilibrated at  $-60 \text{ °C}$  for 2 min then raised to  $100 \text{ °C}$  at a rate of  $4 \text{ °C/min}$ . The effect of temperature on the elastic modulus ( $E'$ ) and on the glass transition temperature was evaluated from the DMA testing and they were reported in Figs. 3 and 4.

2.3.4. In vitro evaluation of cytotoxicity

In vitro biocompatibility studies of photocrosslinked systems

network were performed by indirect method and using Alamar blue test to assess cell Viability. The cells were cultured with the material extracts as below. Extracts for indirect test were obtained from the material under standardized conditions (ISO 10993-5). First, extraction media were prepared by immersing samples cut from photocrosslinked film (about 10 mm in diameter and 1 mm in thickness) in wells of a 24-well culture plate in complete medium following a 100:2,5 (mg/ml) relation. The complete medium with the material was incubate at 37 C and occasionally agitated. After 3 and 5 days of incubation, the extracts were tested with the cell

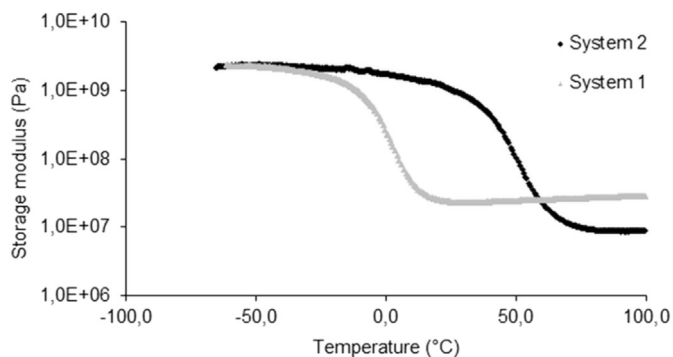


Fig. 3. The storage moduli of the two systems as a function of temperature under three-point flexure at the frequency of 1 Hz.

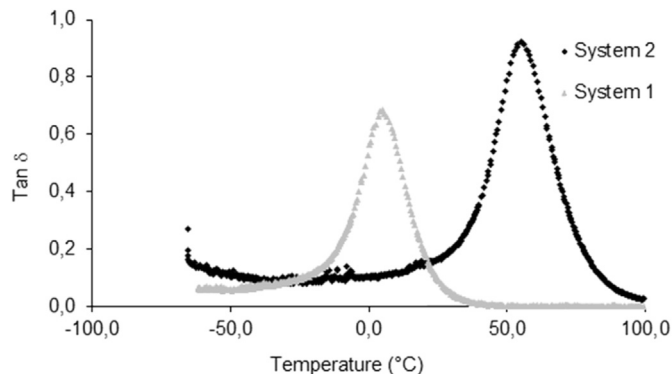


Fig. 4. The tan  $\delta$  of system 1 and system 2 as a function of temperature under three-point flexure at the frequency of 1 Hz.

cultured. For the evaluation of the extracts effect, human osteoblast were seeded in 48-well plate at a density of  $2 \cdot 10^4$  cells per well in 500  $\mu$ l medium. 5 wells were used as blank control. Afterwards the cells were incubated for 24 h and their viability was then established by Alamar Blue test (AB test). AB was added to the samples (10% v/v of medium) and incubated at 37 °C for 3 h. The absorbance of the samples was measured using a spectrophotometer plate reader (Multilabel Counter, 1420 Victor, Perkin Elmer) at 570 nm and 600 nm. AB is an indicator dye that incorporates an oxidation-reduction indicator that changes colour in response to the chemical reduction in growth medium, resulting from cell viability. Difference in percentage of reduction between treated and control cells are calculated with the following equation:

$$\%Reduction = \frac{(O_2 \cdot A_1) - (O_1 \cdot A_2)}{(O_2 \cdot P_1) - (O_1 \cdot P_2)} \cdot 100$$

where  $O_1$  is the molar extinction coefficient (E) of oxidized Alamar Blue at 570 nm;  $O_2$  is the E of oxidized Alamar Blue at 600 nm;  $A_1$  is the absorbance of test wells at 570 nm;  $A_2$  is the absorbance of test wells at 600 nm;  $P_1$  is the absorbance of positive growth control well at 570 nm;  $P_2$  is the absorbance of positive growth control well at 600 nm.

### 2.3.5. Surface functionalization

Mechanical and molecular stimuli from the microenvironment determine gene expression alterations and cell morphology changes such as cell tension (Wang et al., 2002), cell adhesion (Choquest et al., 1997; Beningo et al., 2001), protein expression (Cukierman et al., 2001), cytoskeletal organization (Cukierman et al., 2001; Engler et al., 2004a), and even cell viability (Wang et al., 2000). For this purpose, we tested the adhesion propensity and the correct elongation of a murine myoblast precursors (C2C12) cell line functionalizing the biomaterials (system 1 and system 2) with Fetal Bovine Serum (FBS) or Methanol (MeOH). We decide to functionalize the biomaterials with FBS because it is the most widely used serum-supplement in vitro cell cultures; it contains a very low level of antibodies and more growth factors, hormones, vitamins and proteins such as creatinin and albumin that can support the cell adhesion. Methanol instead has been chosen for its capability to convert hydrophobic membranes such as polyvinylidene difluoride (PVDF) in hydrophilic structures. Treatment with aqueous solution and methanol (1:1) is essential to induce a  $\beta$ -sheet secondary structure of electrospun silk nanofibers.

### 2.3.6. Water contact angle measurements (WCA)

The wettability of the systems, were determined at room temperature by water contact angle goniometry using an OCA measuring instruments (DataPhysics Instruments GmbH) using as test liquids doubly distilled water. Drops (1  $\mu$ l) of liquids were placed on the network surfaces using an end-flat micrometric syringe (Gilmont Instruments, Barrington, IL, USA). At least six drops per liquid and surface condition were measured and averaged and they were reported in Fig. 5.

### 2.3.7. Cells material interactions

Murine myoblast precursors anchorage to substrate and reorganize their cytoskeleton to form contractile myotubes when cultured in optimal conditions. Biomaterials generated into this study were incubated with 100% FBS or absolute MeOH for 1 h and the solutions were washed out with Phosphate Buffered Saline (PBS) (Sigma, USA) for three times. Subsequently, the supports were air dried and sterilized with UV light for 1 h in sterility condition. After 24 h,  $2 \times 10^5$  cells/cm<sup>2</sup> were plated on supports and cultured for 48 h in D-MEM (Gibco, USA) supplemented with heat-

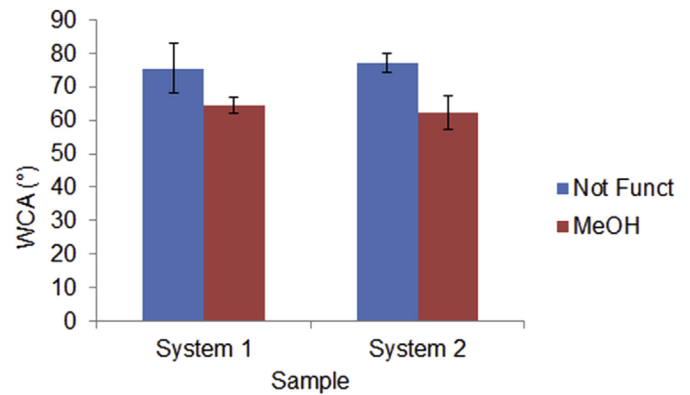


Fig. 5. Results of Alamar blue assay for system 1 and system 2 after 3 and 5 days of immersion in complete medium.

inactivated 10% fetal bovine serum (FBS) (Gibco, USA), GlutaMAX (Gibco, USA) and 100 international units/ml penicillin and 100 mg/ml streptomycin (EuroClone S.p.a., Italy). Then, the biomaterials were washed with PBS for two times and fixed in 4% of paraformaldehyde (PFA). We analysed the adherent cells by a contrast phase microscopy.

### 2.3.8. Myoblast spreading and elongation

Cell spreading was evaluated as cell area using ImageJ cell perimeter tool. Myoblasts elongation was measured as the ratio between major and minor axis of cells. These parameters were calculated in contrast phase images at 20 $\times$  magnification.

## 3. Results and discussions

Polymer networks based on MMA and BMA monomers have potential for a broad range of thermo-mechanical properties. In order to understand the role of the various components used, two different solutions were used (as reported in Table 1) to synthesize a diverse set of polymer networks. Networks properties were determined by studying their thermo-mechanical transitions and stress-strain response for systematically varied monomer functionalities, concentrations, and chemistries. Chain backbone stiffness (capacity for conformational motion) and cohesive energy between chains are the primary drivers for  $T_g$ , but crosslinking and other factors also participate [36].

Fig. 2 shows the DSC plots of each sample labelled as System 1 and 2. The values of glass transition temperature are presented in Table 2. The shift of  $T_g$  to higher temperatures, as shown in Table 2, is related to the higher amount of PMMA in system 2. Butyl methacrylate present a longer side group in the chain and the difference of  $T_g$  between system 1 and system 2 may be expected based on the reduction of steric hindrance to conformational motion from methylene to ester group. PMMA has a  $T_g$  higher than PBMA and this leads to an improvement in a reduced mobility of the chains at room temperature [38]. To quantify the effect of composition on the mechanical properties of the photocrosslinked network, tensile test and dynamical mechanic analysis were conducted. Isothermal tensile stress-strain properties were measured for the materials to quantify relevant mechanical properties such as elastic modulus ( $E'$ ), failure strain ( $\sigma_{max}$ ) and elongation at break ( $\epsilon_{max}$ ). Tensile test show that the elastic modulus and the elongation at break of the network increases from 32 to 260 MPa changing the composition of the resin. The maximum tensile strength and the maximum strain at break increase from 2,78 MPa to 8% to

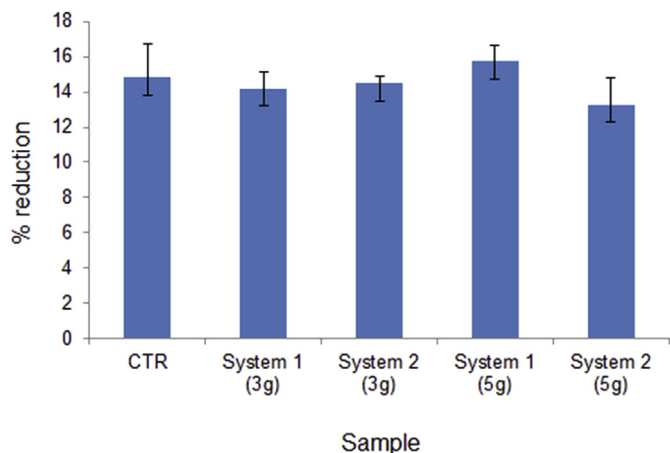


**Fig. 6.** Water contact angle (WCA) for unfunctionalized and Me(OH) threatened surfaces of system 1 and system 2.

10.81 MPa and 40% respectively. Modifying the resin composition, in particular increasing the amount of PEGDA from 8% of system 2–35% of system 1 the network dramatically change his mechanical behaviour. This behaviour showed that mechanical properties strongly depends from the resin composition. In particular the highest presence of MMA in system 2 provides a more rigid network. Moreover the results of elongation at break ( $\epsilon_{max}$ ) of the two systems shows that the higher the amount of PEGDA, the lower is the elongation at break and this can explain the quasi-brittle behaviour of system 1.

Photo-crosslinked films were subjected to dynamic mechanical analysis. Temperature sweeps were performed at fixed frequency of 1 Hz, and resulting storage modulus and  $\tan\delta$  measurements were plotted to yield the curves shown in Figs. 3 and 4. Fig. 3 illustrates the storage moduli of the two systems as a function of temperature at the frequency of 1 Hz. The storage modulus in DMA is related to the stiffness of material. At low temperatures, the storage moduli of the two samples do not show significant difference. However, when the temperature increases (between 0 and 50 °C), system 2 exhibits higher storage modulus. The values of E determined by stress–strain testing are consistent with the values of storage modulus

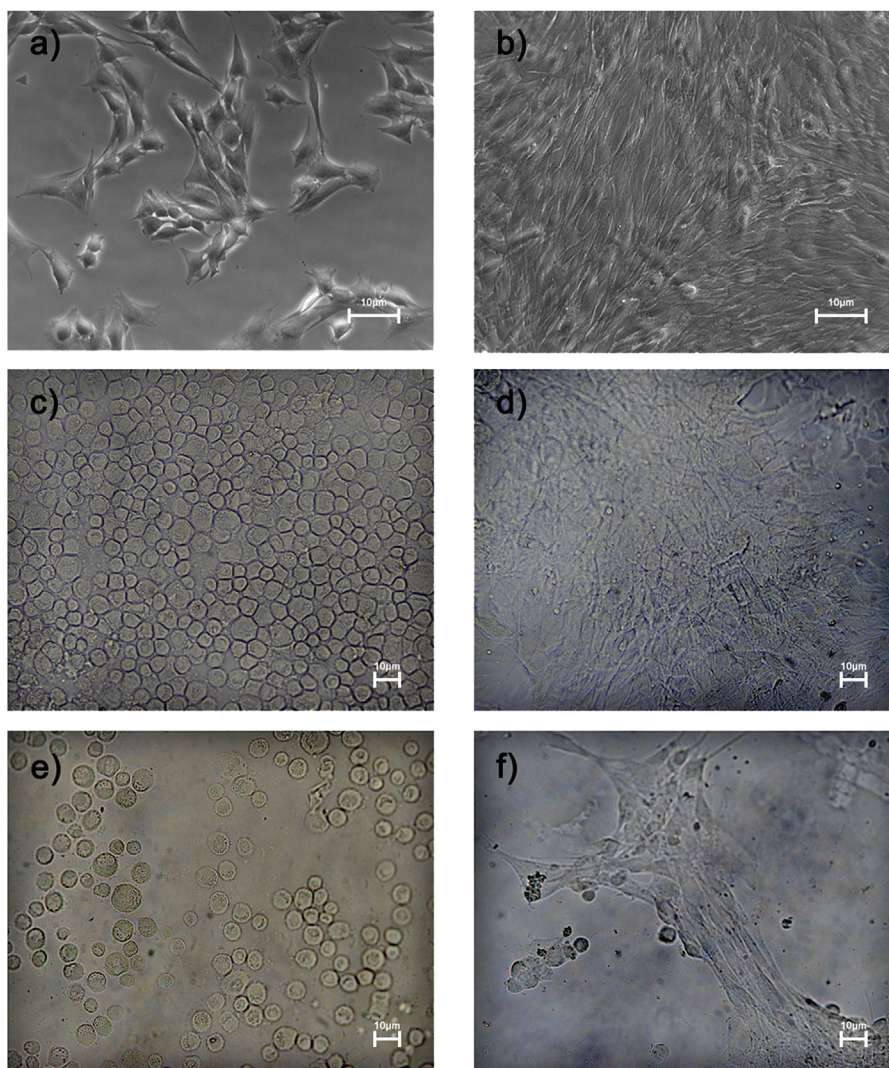


**Fig. 7.** Representative images of murine myoblast precursors. C2C12 cell line plated to low density on normal dish show their characteristic morphology (a). Myoblasts to high confluence begin to fuse into nascent myotubes (b). Cells plated on system 1 and system 2 functionalized with FBS showed low affinity to substrates and preserved their immature round shape (c,e). Instead, biomaterials pre-treated with MeOH promoted myoblasts fusion and correct myotubes formation, similarly to standard cell cultures on plastic dishes (d,f). (White bar represent 10 µm).

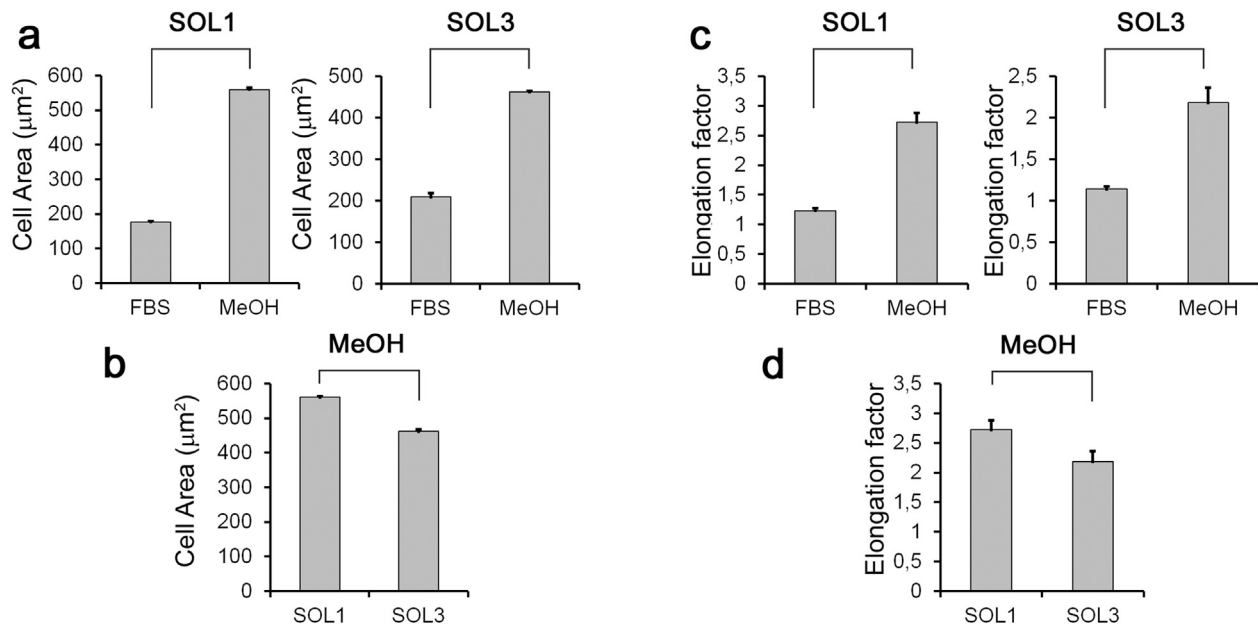


**Fig. 8.** Myoblasts responses to different functionalization. a) Cell spread area increases by MeOH functionalization in both system 1 and system 2 biomaterials compared to FBS,  $p < 0.01$ . b) system 1 increases cell spreading index respect to system 2 after MeOH functionalization,  $p < 0.05$ . c) Elongation factor, calculated as ratio of the cells major axis to its minor axis, is enhanced following MeOH functionalization in both system 1 and system 2 biomaterials compared to FBS,  $p < 0.01$ . d) system 1 increases elongation factor respect to system 2 after MeOH functionalization,  $p < 0.05$ .

determined by three-point bend testing of the dynamic mechanical analysis at the same temperatures as showed in Table 2.

The Comparison of the mechanical properties suggests that system 1 is a better candidate than system 2 for bone tissue engineering due to its higher Young modulus and higher elongation at break which makes it suitable for load bearing applications such as trabecular bone of the tibia plateau [39].

Understanding the effect of materials composition and processing at the cellular level is crucial to optimising the use of the materials *in vivo*. One way to investigate the early interaction between system 1 and 2 and living cells is to study the *in vitro* cytotoxicity. Cytotoxicity testing is the initial phase in testing biocompatibility of biomaterials. Using an *in vitro* system, it is possible to assess if the initial dissolution of the material surface might be associated with undesirable cellular effect. Cytotoxicity assay were based on the exposition of human cells to liquid extract of system 1 and 2 to study the possible toxic substance leached from the biomaterials. Complete liquid culture medium has been considered as negative or non-toxic control. For each materials the complete medium has been extracted after 3 and 5 days of incubation and tested with the cultured cell. Cell viability was investigated by alamar blue assay [37]. Cell viability and proliferation were evaluated using the alamar blue assay. This is based on a redox reaction that occurs in the mitochondria of the cells. The coloured product is transported out of the cell and can be measured spectrophotometrically. Results, presented in Fig. 5, demonstrate that extract of system 1 and system 2 showed almost no cytotoxic effect when tested on human osteoblast. In addition few changes in cell viability were observed in function of the time of extraction. This experiment demonstrate that extract of system 1 and system 2 do not show any significant cytotoxic effect and confirm biocompatibility of this materials.

WCA was measured at room temperature using an OCA 20 Contact Angle Analyzer. Spot WCA measurements made on different areas of treated and untreated system 1 and system 2 showed a good degree of variability. An average of 8–10 spot measurements per sample were made and the WCA profiles

obtained before and after the treatment with Me(OH) were compared. Within the group of tested network system 1 and system 2 showed similar values of contact angles confirming that both materials have a hydrophobic behaviour, with a water contact angle higher than  $75^\circ$  as reported in Fig. 5. Even if the higher amount of PEGDA in system 1 results in a small decrease of WCA compared to system 2 it remain still higher with value over  $70^\circ$ . This means that the material is still unsuitable for tissue engineering purpose. The treatment with methanol seems to change the surface properties of both network and the WCA decreases from  $75^\circ$  to  $62^\circ$  for system 1 and from  $78^\circ$  to  $63^\circ$  for system 2 as shown in Fig. 6.

Mechanical and molecular stimuli from the microenvironment determine gene expression alterations and cell morphology changes such as cell tension [40], cell adhesion [41], protein expression [42], cytoskeletal organization [42] [43], and even cell viability [44]. For this purpose, we tested the adhesion propensity and the correct myotubes formation of a murine myoblast precursors (C2C12) cell line functionalizing the biomaterials (system 1 and system 2) with FBS or MeOH. We analysed the adherent cells by a contrast phase microscope (Fig. 6). Cells plated on system 1 and system 2 functionalized with FBS showed low affinity to substrates and preserved their immature round shape (Fig. 7 c; e). Instead, biomaterials pre-treated with MeOH promoted myoblasts adhesion and fusion, similarly to standard cell cultures on plastic dishes (Fig. 7 d; f).

Myoblasts spread area increased in both biomaterials functionalized with MeOH compared to FBS (Fig. 8a), but cell spreading index in system 1 is improved respect to system 2 (Fig. 8b). Myoblasts elongation is also enhanced after MeOH functionalization in both system 1 and system 2 (Fig. 8c), but system 1 promoted cell elongation respect to system 2 (Fig. 8d). We may conclude that both FBS or MeOH functionalization of network surface allow cell adhesion and survival, but the MeOH pre-treatment only promotes spreading, elongation, fusion and myotubes formation of C2C12 muscular precursor cells plated on system 1 and system 2 surfaces.

#### 4. Conclusions

In this work photo-crosslinkable resins based on MMA, BMA and PEGDA as crosslinker was developed and characterized in terms of mechanical, thermal and biological behaviour. The starting idea was the improvement of mechanical and biological characteristic of the PMMA by the realization of different copolymer. Two system have been analysed modifying the relatively amount of each component. The use of BMA and PEGDA strongly influenced the mechanical behaviour especially in terms of elastic modulus and elongation at break. Cytotoxicity test show that both system 1 and system 2 do not show any significant cytotoxic effect and confirm biocompatibility of this materials. However even if system 1 and system 2 showed almost no cytotoxic effect when tested on human osteoblast the material still have a lack of biological recognition by the cell due its poor wettability and absence of specific biological signals. Two different surface treatments with FBs or MeOH have been developed in order to improve the cell recognition of materials surface. For this purpose C2C12 murine myoblast precursors cells have been tested in terms of adhesion and spreading propensity. Preliminary test of the samples treated with MeOH showed that materials promote myoblasts fusion and correct myotubes formation, similarly to standard cell cultures on plastic dishes. The good mechanical and biological performance of the proposed network, and the high reactivity of the resin demonstrates that the material proposed will be well suited for stereolithography application in tissue engineering.

#### References

- [1] J.M. Karp, P.D. Dalton, M.S. Shoichet, Scaffolds for tissue engineering, *MRS Bull.* 28 (2003) 301–306.
- [2] D.W. Huttmacher, Scaffolds in tissue engineering: bone and cartilage, *Biomaterials* 21 (2000), 2529–3254.
- [3] K.J. Rambahia, P.X. Ma, Controlled drug release for tissue engineering, *J. Control. Releas.* 219 (2015) 119–128.
- [4] J.S. Temenoff, A.G. Mikos, Injectable biodegradable materials for orthopedic tissue engineering, *Biomaterials* 21 (2000) 2405–2412.
- [5] H. Eufinger, M. Wehmoller, A. Harders, L. Heuser, Prefabricated prostheses for the reconstruction of skull defects, *Int. J. Oral. Maxillofac. Surg.* 24 (1995) 104–110.
- [6] S.C. Lee, C.T. Wu, S.T. Lee, P.J. Chen, Cranioplasty using polymethyl methacrylate prostheses, *J. Clin. Neurosci.* 16 (2009) 56–63.
- [7] P. Frutos Cabanillas, E. Diez Peña, J.M. Barrales-Rienda, G. Frutos, Validation and in-vitro characterization of antibiotic-loaded bone cement release, *Int. J. Pharm.* 209 (2000) 15–26.
- [8] M.H. Pelletier, L. Malisano, P.J. Smitham, K. Okamoto, W.R. Walsh, The compressive properties of bone cements containing large doses of antibiotics, *J. Arthroplast.* 24 (2009) 454–461.
- [9] A. Ronca, S. Ronca, G. Forte, S. Zeppetelli, A. Gloria, R. De Santis, L. Ambrosio, Synthesis and characterization of divinyl-fumarate Poly-ε-caprolactone for scaffolds with controlled architectures, *J. Tissue Eng. Regen. Med.* 10.1002/term.2322.
- [10] R. De Santis, A. Gloria, T. Russo, A. Ronca, U. D'Amora, G. Negri, D. Ronca, L. Ambrosio, Viscoelastic properties of rapid prototyped magnetic nano-composite scaffolds for osteochondral tissue regeneration, *Procedia CIRP* 49 (2016) 76–82.
- [11] A. Gloria, T. Russo, R. De Santis, L. Ambrosio, 3D fiber deposition technique to make multifunctional and tailor-made scaffolds for tissue engineering applications, *JABB* 7 (2009) 141–152.
- [12] A. Ronca, L. Ambrosio, D.W. Grijpma, Design of porous three-dimensional PDLLA/nano-hap composite scaffolds using stereolithography, *J. Appl. Biomater. Funct. Mater* 10 (2012) 249–258.
- [13] J. Chai, F. Lu, B. Li, D.Y. Kwok, Wettability interpretation of oxygen plasma modified poly(methyl methacrylate), *Langmuir* 20 (2004) 10919–10927.
- [14] D. Espalin, K. Arcaute, D. Rodriguez, F. Medina, Fused deposition modeling of patient-specific polymethylmethacrylate implants, *Rapid Prototyp. J.* 16 (3) (2010) 164–173.
- [15] R. De Santis, F. Mollica, L. Ambrosio, L. Nicolais, D. Ronca, Dynamic mechanical behavior of PMMA based bone cements in wet environment, *J. Mater. Sci. Mater. Med.* 14 (2003) 583–594.
- [16] R. De Santis, A. Gloria, D. Ronca, G. Guida, L. Nicolais, L. Ambrosio, Structural and mechanical properties of the cement-bone composite, *JAAB* 4 (2006) 194.
- [17] J.P. Davies, W.H. Harris, Comparison of diametral shrinkage of centrifuged and uncentrifuge simplex P® bone cement, *J. Appl. Biomater.* 6 (1995) 209–211.
- [18] S.S. Haas, G.M. Brauer, G. Dickson, A characterization of polymethylmethacrylate bone cement, *J. Bone Jt. Surg.* 57A (1975) 380–391.
- [19] H.W. Hamilton, D.F. Cooper, M. Fels, Shrinkage of centrifuged cement, *Orthop. Rev.* 17 (1988) 48–54.
- [20] J.L. Gilbert, J.M. Hasenwinkel, R.L. Wixson, E.P. Lautenschlager, A theoretical and experimental analysis of polymerization shrinkage of bone cement: a potential major source of porosity, *J. Biomed. Mater. Res.* 52 (2000) 210–218.
- [21] C.D. Jefferis, A.J.C. Lee, R.S.M. Ling, Thermal aspects of self-curing poly(methyl methacrylate), *J. Bone Jt. Surg.* 57B (1975) 511–518.
- [22] A. Borzacchiello, L. Ambrosio, L. Nicolais, D. Ronca, G. Guida, The temperature at the bone-cement interface: modelling and “in vitro” analysis, in: Francesco Pipino (Ed.), *Bone Cement and Cemented Fixation of Implant*, 2001, pp. 135–140.
- [23] P.A. Revell, M. Braden, M.A.R. Freeman, Review of the biological response to a novel bone cement containing poly(ethyl methacrylate) and n-butyl methacrylate, *Biomater* 19 (1998) 1579–1586.
- [24] P.A. Revell, M. Freeman, B. Weightman, B. Braden, The intra-osseous implantation of a new bone cement polyethylmeth-acrylate/n-butyl methacrylate in the dog, in: *Proc. Fourth World Biomaterials Congress, Berlin, 1992*, p. 166.
- [25] B.J. Mondino, S. Nagata, M.M. Glovsky, Activation of the alternative complement pathway by intraocular lenses, *Investig. Ophthalmol. Vis. Sci.* 26 (1985) 905–908.
- [26] B.J. Mondino, G.M. Rajacich, H. Sumner, Comparison of complement activation by silicone intraocular lenses and polymethylmethacrylate intraocular lenses with polypropylene loops, *Arch. Ophthalmol.* 105 (1987) 989–990.
- [27] K. Miyake, M. Asakura, H. Kobayashi, Effect of intraocular lens fixation on the blood-aqueous barrier, *Am. J. Ophthalmol.* 98 (1984) 451–455.
- [28] R. Li, I. Ye, Y.W. Mai, Application of plasma technologies in fibre-reinforced polymer composites: a review of recent developments, *Compos. Part A Appl. Sci. Manuf.* 28A (1997) 73–86.
- [29] G. Lewis, Properties of acrylic bone cement: state of the art review, *J. Biomed. Mater. Res. A* 38 (1997) 155–182.
- [30] C. Ohtsuki, T. Miyazaki, M. Kyomoto, M. Tanihara, A. Osaka, Development of bioactive PMMA based cement by modification with alkoxysilane and calcium salt, *J. Mater. Sci. Mater. Med.* 12 (2001) 895–899.
- [31] A.M. Moursi, A.V. Winnard, P.L. Winnar, J.J. Lannutti, R.R. Seghi, Enhanced osteoblast response to a Polymethyl methacrylate–hydroxyapatite composite, *Biomaterials* 23 (2002) 133–144.
- [32] T.G. van Kooten, J.M. Schakenraad, H.C. van der Mei, H.J. Busscher, Influence of substratum wettability the strength of adhesion of human fibroblasts, *Biomaterials* 13 (1992) 897–904.
- [33] J.M. Schakenraad, H.J. Busscher, C.R.H. Wildevuur, J. Arends, The influence of substratum surface free energy on growth and spreading of human fibroblasts in the presence and absence of serum proteins, *J. Biomed. Mater. Res.* 20 (1986) 773–784.
- [34] D.R. Absolom, L.A. Hawthorn, G. Chang, Endothelialization of polymer surfaces, *J. Biomed. Mater. Res.* 22 (1988) 271–285.
- [35] P.B. Van Wachem, T. Beugeling, J. Feijen, A. Bantjes, J.P. Detmers, W.G. Van Aken, Interaction of cultured human endothelial cells with polymeric surfaces of different wettabilities, *Biomaterials* 6 (1985) 403–408.
- [36] J. Bicerano, *Prediction of Polymer Properties*, 1996. New York.
- [37] M.G. Raucchi, V. D'Antò, V. Guarino, E. Sardella, S. Zeppetelli, P. Favia, L. Ambrosio, Biomaterialized porous composite scaffolds prepared by chemical synthesis for bone tissue regeneration, *Acta Biomater.* 6 (2010) 4090–4099.
- [38] M. Leskovic, V. Kovacevic, D. Fles, D. Hace, Thermal stability of poly(methyl methacrylate-co-butyl acrylate) and poly(styrene-co-butyl acrylate) polymers, *Polym. Eng. Sci.* 39 (1999) 600–608.
- [39] D. Ronca, A. Gloria, R. De Santis, T. Russo, U. D'Amora, M. Chierchia, L. Nicolais, L. Ambrosio, Critical analysis on dynamic-mechanical performance of spongy bone: the effect of an acrylic cement, *Hard Tissue* 3 (2014) 9.
- [40] N. Wang, I.M. Tolić-Nørrelykke, J. Chen, S.M. Mijailovich, J.P. Butler, J.J. Fredberg, D. Stamenović, Cell prestress. I. Stiffness and prestress are closely associated in adherent contractile cells, *Am. J. Physiol. Cell. Physiol.* 282 (2002) 606–616.
- [41] D. Choquet, D.P. Felsenfeld, M.P. Sheetz, Extracellular matrix rigidity causes strengthening of integrin-cytoskeleton linkages, *Cell* 88 (1997) 39–48.
- [42] E. Cukierman, R. Pankov, D.R. Stevens, K.M. Yamada, Taking cell-matrix adhesions to the third dimension, *Science* 294 (2001) 1708–1712.
- [43] A.J. Engler, M.A. Griffin, S. Sen, C.G. Bönnemann, H.L. Sweeney, D.E. Discher, Myotubes differentiate optimally on substrates with tissue-like stiffness: pathological implications for soft or stiff microenvironments, *J. Cell Biol.* 166 (2004) 877–887.
- [44] H.B. Wang, M. Dembo, Y.L. Wang, Substrate flexibility regulates growth and apoptosis of normal but not transformed cells, *Am. J. Physiol. Cell Physiol.* 279 (2000) 1345–1350.